

BFO films obtained by Spray Pyrolysis optical and structural analysis

Análisis óptico y estructural de películas de BFO obtenidas por Spray Pirólisis

HERNÁNDEZ-SIMÓN, Zaira Jocelyn†, LUNA-LÓPEZ, José Alberto*, HERNÁNDEZ-DE LA LUZ, Álvaro David and MENDOZA-CONDE, Gabriel Omar

Centro de Investigaciones en Dispositivos Semiconductores (CIDS-ICUAP), Benemérita Universidad Autónoma de Puebla (BUAP), Col. San Manuel, Cd. Universitaria, Av. San Claudio y 14 Sur, Edificios IC5 y IC6, Puebla, Pue., 72570, México.

ID 1st Author: Zaira Jocelyn, Hernández-Simón / ORC ID: 0000-0003-4185-4101, CVU CONACYT ID: 774431

ID 1st Co-author: José Alberto, Luna-López / ORC ID: 0000-0002-7647-3184, CVU CONACYT ID: 200808

ID 2nd Co-author: José Álvaro David, Hernández-de la Luz / ORC ID: 0000-0002-7913-0240, CVU CONACYT ID: 240901

ID 3rd Co-author: Gabriel Omar, Mendoza-Conde / ORC ID: 0000-0001-5451-9770, CVU CONACYT ID: 774931

DOI: 10.35429/EJT.2022.11.6.28.34

Received January 20, 2022; Accepted June 30, 2022

Abstract

In the present research work, the obtaining of BiFeO₃ films using the ultrasonic Spray Pyrolysis technique is reported. The deposited films were characterized optically and structurally, showing interesting results, such as the formation of column-type microstructured arrangements with an average height of 805 nm, as well as the presence of 2 predominant phases in the material, the combination of rhombohedral BiFeO₃ with tetragonal Bi₂O₃, in addition to the tetragonal Bi₃₆Fe₂O₅₇ phase. From the diffraction patterns, the lattice parameters were also obtained, with which the crystalline structure of each phase was graphically represented, the average crystallite size was calculated using the Scherrer formula with an average size of 13 nm, which could benefit the Magnetic properties of BiFeO₃. The film also shows a band gap shift at lower energies, which is an improvement for future applications in the field of photovoltaics, furthermore these films were obtained with a simple and economical technique using a deposition temperature of only 100°C.

BiFeO₃, Structural characterization, Spray pyrolysis

Resumen

En el presente trabajo de investigación se reporta la obtención de películas de BiFeO₃ utilizando la técnica de Spray Pyrolysis ultrasónico, las películas depositadas fueron caracterizadas óptica y estructuralmente mostrando resultados interesantes, como la formación de arreglos microestructurados de tipo columna con una altura promedio de 805 nm, así como la presencia de 2 fases predominantes en el material, la combinación de BiFeO₃ romboédrico con Bi₂O₃ tetragonal, además de la fase Bi₃₆Fe₂O₅₇ tetragonal. De los patrones de difracción también fueron obtenidos los parámetros de red, con lo cual se representó gráficamente la estructura cristalina de cada fase, los tamaños de cristalito promedio fueron calculados utilizando la fórmula de Scherrer con tamaños promedio de 13 nm, lo cual podría beneficiar las propiedades magnéticas del BiFeO₃. La película, además, muestra un corrimiento del band gap a menores energías, lo cual es beneficioso para futuras aplicaciones en el campo de la fotovoltaica, además estas películas fueron obtenidas con una técnica sencilla y económica usando una temperatura de depósito de sólo 100°C.

BiFeO₃, Caracterización estructural, Spray Pirolisis

Citation: HERNÁNDEZ-SIMÓN, Zaira Jocelyn, LUNA-LÓPEZ, José Alberto, HERNÁNDEZ-DE LA LUZ, Álvaro David and MENDOZA-CONDE, Gabriel Omar. BFO films obtained by Spray Pyrolysis optical and structural analysis. ECORFAN Journal-Taiwan. 2022. 6-11: 28-34.

* Correspondence to Author (E-mail: jose.luna@correo.buap.mx)

† Researcher contributing as first author.

Introduction

As well known, multiferroics are interesting materials which exhibits at least two of the ferroic properties in the same phase and exhibit a coupling effect between the ferroic properties [1].

Among many ferroelectric materials, BiFeO₃ (BFO) is one of the key research materials due to its large remanent polarization (~100 μC/cm²), high Curie temperature (~810 °C) and narrow direct band gap (~2.7 eV) [2], whereby it has significant absorption of visible light, which is beneficial for the development of solar energy devices [3]. Nevertheless, the major challenge on BiFeO₃ based photovoltaic devices is low photovoltaic output, which is affected by their intrinsic ferroelectric photovoltaic mechanism [4].

Besides to photovoltaic applications, the BFO has also applications in the field of spintronics, sensors and new data storage devices. [5].

Many physical and chemical methods have been used to obtain BFO films, including radio-frequency sputtering, molecular beam epitaxy, pulsed laser deposition, chemical (sol-gel) solution deposition, and hydrothermal synthesis, have been employed for the deposition of BFO thin films. Notwithstanding, these deposition techniques are highly expensive, and it is required long time for deposition process. On the other hand, spray pyrolysis is a very simple and inexpensive deposition technique for thin films fabrication, and it has potential for large scale preparation. Additionally, precise control of composition and better chemical homogeneity are possible in this deposition technique [6].

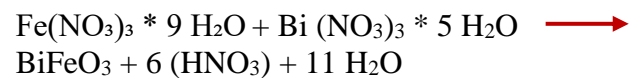
The growing condition which allows a pure and stoichiometric BFO phase to be obtained is always very narrow, so that very small changes in the deposition parameters can lead to either major changes in the film's properties or to the nucleation of spurious phases. The BFO films have been reported to present a magnetic moment arising from parasitic phases formed mainly by iron oxides [7].

In the case of impurity phases that present an excess of bismuth, such as Bi₂₅FeO₃₉ or the combination of BFO with B₂O₃, a great interest has recently arisen in their formation, due to investigations that report the superior photocatalytic action that they exhibit [8] along with good photoelectric response.

Description of the method

The BFO films were deposited using the Spray Pyrolysis technique, the deposit temperature used was 100°C and for preparing the precursor solution a molarity of 0.6 M was used, it was required as a first step to use a reaction for which the following reagents were used; Iron nitrate nonahydrate 98% and Bismuth Nitrate pentahydrate

Causing the following reaction:



The deposition time used was 10 minutes and the deposition were carried out on an n-type silicon substrate with a resistivity of 1-10 Ω, orientation (1 0 0), the deposit distance between the hot wall and the substrate was 4 cm.

After the deposit, a thermal annealing of 500°C was carried out in accordance with what was reported by [9], in that investigation annealing at higher temperatures was carried out, resulting in the emergence of phases Bi₂Fe₄O₉ and Bi₂₅FeO₃₉ at 700°C temperature and at temperatures higher than 800°C there is a decrease in the phase Bi₂₅FeO₃₉ and the phase Bi₂Fe₄O₉ becomes dominant.

To structurally characterize the obtained film, profilometry measurements were made in a Dektak 150 profilometer with a vertical tracking resolution of 1 Å, SEM measurements were also made with a JEOL JSM-5300 equipment applying 20kV. Finally, grazing incidence X-ray diffraction measurements, with an angle θ-2θ of 1° using a Bruker D8 Venture equipment was carried out.

To obtain the optical properties of the material, diffuse reflectance and absorbance measurements were made using a Varian Cary 5000 UV-Vis-NIR spectrophotometer. Finally, the obtained structures were modeled using the Diamond 4 Cristal and molecular structure visualization software.

Results

In Figure 1, a photograph of the appearance of the film obtained without close-ups is presented in the upper left part, while in the lower part a photograph of the film taken with microscope magnification is shown with the presence of small clusters within the film.

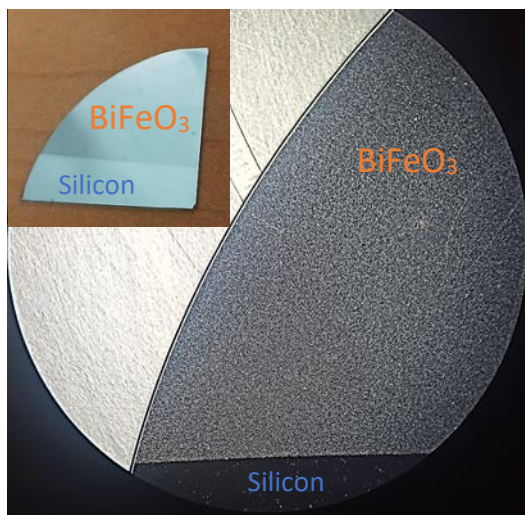
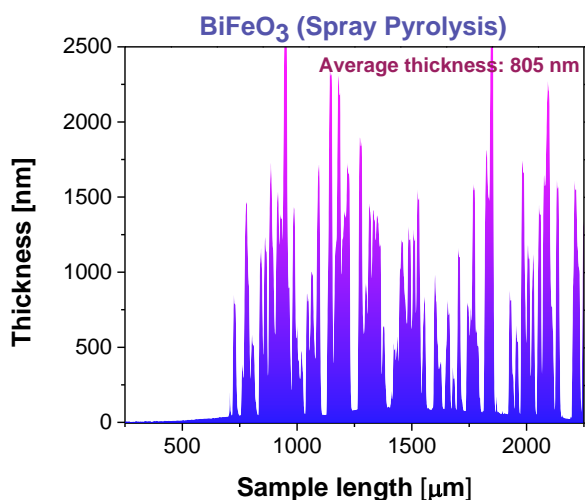


Figure 1 Image of the film obtained using the spray pyrolysis technique

In order to properly analyze the thickness and morphology of the film, Graphic 1 shows the thickness profile obtained by profilometry, where column-type microstructured arrangements with an average height of 805 nm can be observed, the separation among these growths has micron variations where the growth of a thin film of BFO with a thickness of approximately 150 nm is also observed.



Graphic 1 Thickness profile and average thickness for the BFO film deposited by Spray Pyrolysis

Figure 2 present the SEM micrographs obtained from the film, where subsection a) shows the presence of the columns observed by profilometry and their distribution fully coincides with the profile obtained from the sample, also in part b) it is shown a magnification x2000 where these columns have a circular shape with a variable diameter, but with an average of 5 μm .

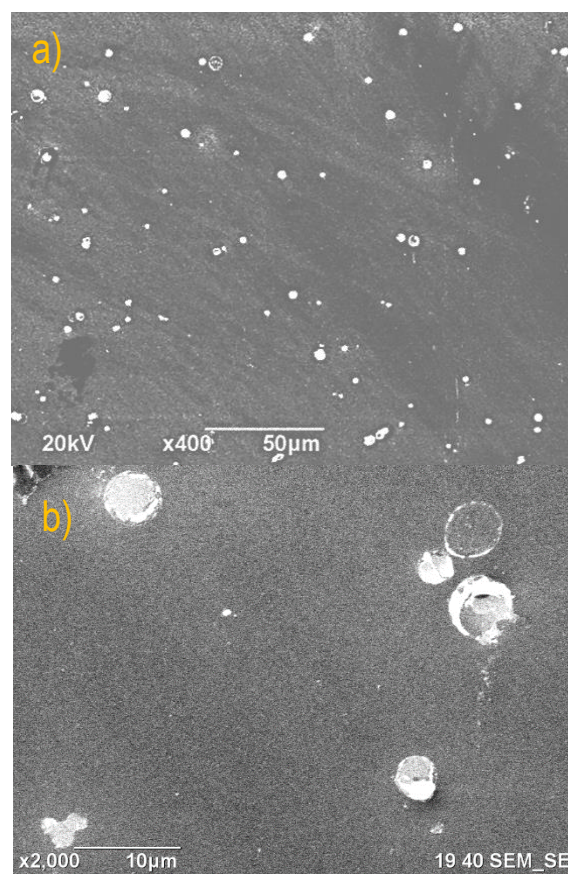
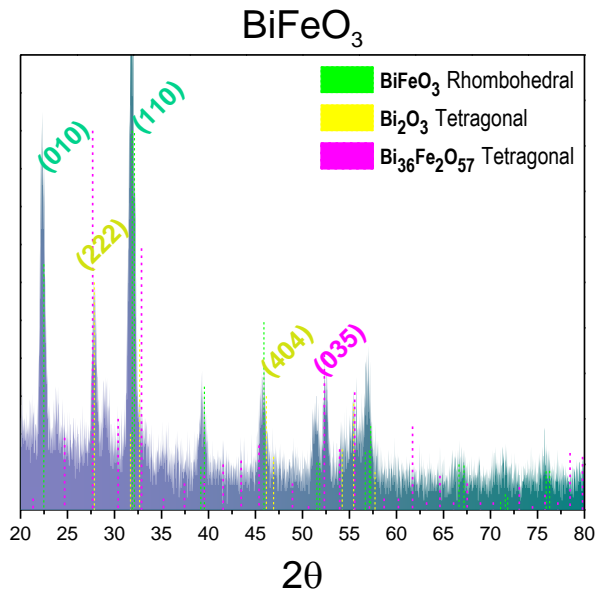


Figure 2 Micrographs of the BFO film obtained by SEM with different magnifications.

Graphic 2 shows the diffraction pattern, where we present the rhombohedral phase of BiFeO_3 with a preferential orientation in the (110) plane, it is also observed that there is a mixture with the tetragonal phase of Bi_2O_3 which presents a preferential orientation in the plane (222).

Both phases present in the film correspond to the structure at room temperature for each case. Finally, the presence of the tetragonal phase of $\text{Bi}_{36}\text{Fe}_2\text{O}_{57}$ with a preferential orientation in the (035) plane is also observed to a lesser extent.



Graphic 2 Diffractogram of BFO deposited by Spray Pyrolysis and diffraction patterns of rhombohedral BiFeO₃, tetragonal Bi₂O₃ and tetragonal Bi₃₆Fe₂O₅₇

Figure 3 shows a structural representation of the phases and materials obtained using the lattice parameters found in the diffraction pattern of the film obtained by spray pyrolysis.

The lattice parameters are as follows:

BiFeO₃ $a = 3.952 \text{ \AA}$, $b = 3.952 \text{ \AA}$, $c = 3.952 \text{ \AA}$ y $\alpha = \beta = \gamma = 89.6^\circ$.

Bi₂O₃ $a = 7.7299 \text{ \AA}$, $b = 7.7299 \text{ \AA}$, $c = 5.6587 \text{ \AA}$ y $\alpha = \beta = \gamma = 90^\circ$.

Bi₃₆Fe₂O₅₇ $a = 10.184 \text{ \AA}$, $b = 10.184 \text{ \AA}$, $c = 10.184 \text{ \AA}$ y $\alpha = \beta = \gamma = 90^\circ$.

From the diffraction pattern, mean crystallite sizes are calculated using the Scherrer's formula from the broadening of the peaks.

Scherrer's formula is:

$$t = \frac{K\lambda}{\beta \cos \theta} \quad (1)$$

Where t is the crystallite size, K is Scherrer's constant (0.94), λ is the wavelength of the radiation source (1.59 Å), β is the full width at half maximum, and θ is the angle of Bragg [10].

The results obtained show an average crystallite diameter of approximately 13 nm for BFO, as well as for Bi₂O₃.

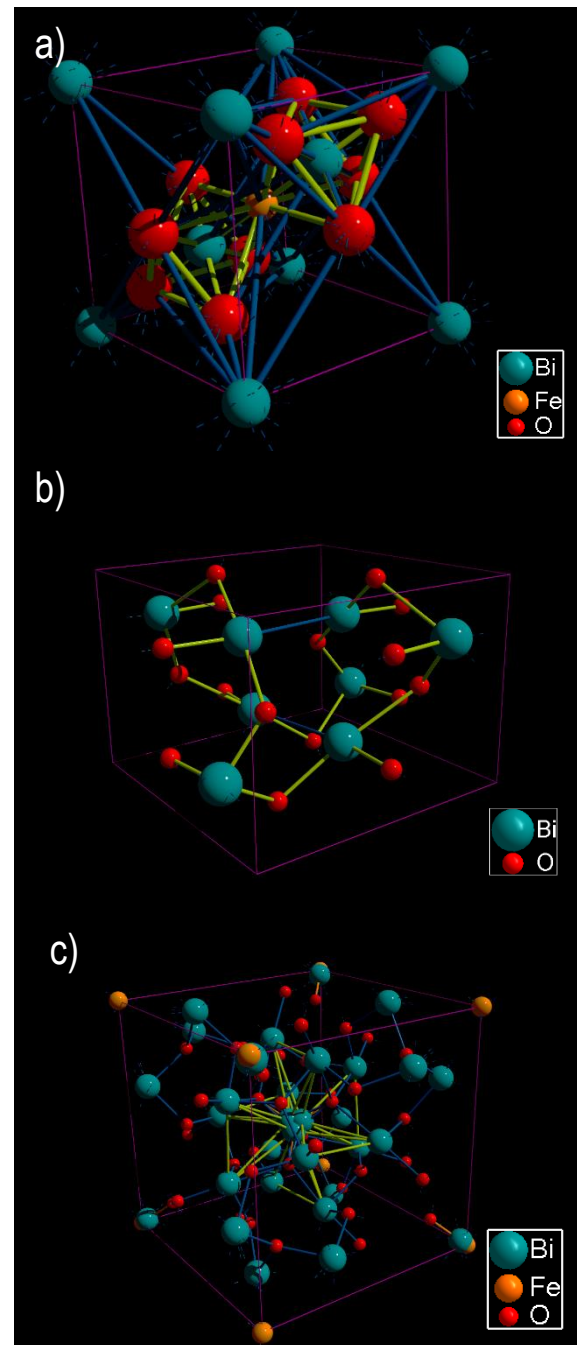
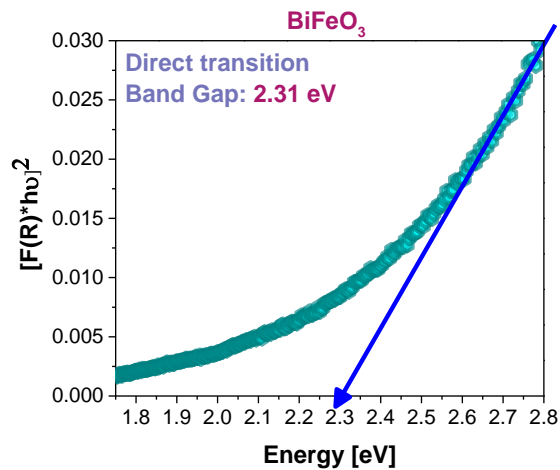


Figure 3 Representation of the different phases present in the obtained film a) BiFeO₃ rhombohedral, b) Bi₂O₃ tetragonal, c) Bi₃₆Fe₂O₅₇ tetragonal

Regarding to the optical properties of the material, Graphic 3 shows the band gap calculated by means of diffuse reflectance measurements and the use of the Kubelka-Munk function [11] where a direct type transition was used in accordance with what was reported for the BFO [12].

The band gap obtained corresponds to 2.31 eV, so there is a shift in the band gap of the material towards lower energies.



Graphic 3 Band gap of the BFO film calculated by the Kubelka-Munk function using a direct transition

Analysis

From the X-ray diffractograms it is observed as mentioned above, that in the film deposit we obtain the rhombohedral phase of BiFeO₃ in combination with the tetragonal phase of Bi₂O₃ and to a lesser extent the Bi₃₆Fe₂O₅₇ in tetragonal phase. Spectra such as the ones obtained have been reported in investigations where the union of BiFeO₃-Bi₂O₃ films is analyzed [13], as well as the heterojunction of nanofibers and other composites of these 2 materials [14]. These results, together with those obtained by SEM, could indicate that a BiFeO₃ film is actually being obtained, so BiFeO₃ is embedded with Bi₂O₃ (clusters or columns observed in figure 2), although according to the size of the crystallites, this mixture of phases could be considered to be at the nanometric level with nanocrystalline embedding. This result is very interesting from the magnetic point of view since it has been reported [12] that the magnetic properties in BFO increase as the crystallite size decreases.

Regarding the Bi₃₆Fe₂O₅₇ phase, it is reported that small amounts of bismuth-rich secondary phases such as Bi₄₀Fe₂O₆₃ and Bi₃₆Fe₂O₅₇ are commonly found in polycrystalline samples of BiFeO₃ and the segregation of these secondary phases at the grain boundaries could play a role in reducing the resistivity of the material. The low resistivity, and resulting low bias inhibit the ferroelectric hysteresis loop [15].

The Bi₃₆Fe₂O₅₇ phase, as well as the Bi₂O₃ phase, indicate an excess of bismuth in our film, which could be explained in terms of the low deposition temperature of 100°C used and the heat annealing carried out at 500°C.

The Bi₂O₃ is a p-type bismuth-based semiconductor with unique physical and chemical characteristics which make it promising in photoelectric applications, it has a band gap of 2.2 to 2.8 eV and shows good absorption in the visible region of the light [14]. According to the results published by [16], BiFeO₃ is a typical n-type semiconductor, so the heterojunction of Bi₂O₃/BiFeO₃ forms a p-n junction type compound, thus the photogenerated charges are effectively separated and transferred at the interface of Bi₂O₃ and BiFeO₃ [14].

Furthermore, a high photovoltaic performance in BiFeO₃ films by manipulating the concentration of their oxygen vacancies through the alteration of the Bi content has been reported, the results of this research show that the highest photovoltaic production was achieved in Bi_{1.05}FeO₃ films, whose response is 1000 times better than that of Bi_{0.95}FeO₃ films, as a charge balance requirement in BFO, Bi vacancies lead to an increase in the oxygen vacancy concentration, while an excess of Bi is linked to a decrease in the oxygen vacancy concentration [17].

Analyzing the shift of the band gap obtained towards lower energies, this can be attributed to the mixture of phases with the insertion of Bi₂O₃ in the BFO molecular structure present in the film, which again corroborates what is observed from the diffractogram of Graph 2, this shift is also beneficial for light absorption according to what was reported in [13] where the decrease in the band gap is obtained by doping the BFO, so in our case the presence of important quantities of Bi₂O₃ molecules causes the reduction of the bandgap energy of the film.

In this context, it is easy to discern that obtaining the reported BiFeO₃-Bi₂O₃ film represents an enormous advantage in terms of materials that are to be applied in the field of photovoltaics (both in solar cells and photocatalytic applications), since it is a film with both phases well defined, besides to the fact that the deposit technique is simple and economical when using the pyrolysis spray system.

Conclusions

In the present research, the obtaining of BiFeO₃-Bi₂O₃ films by means of the ultrasonic Spray Pyrolysis technique is reported, with the formation of 2 phases in the material, namely, BiFeO₃ with a rhombohedral structure and Bi₂O₃ with a tetragonal phase, additionally to the presence of the tetragonal Bi₃₆Fe₂O₅₇ phase, this is indicative of an excess bismuth in the material possibly attributed to the low deposition temperature. Obtaining this type of structures by the ultrasonic Spray Pyrolysis technique is so important for future photoelectric applications due to the various investigations are focused on obtaining this type of arrangement by sophisticated techniques. The reported structures possess an excellent response to light, such fact makes them good candidates to improving photovoltaic cells based on multiferroic materials.

Funding

This work has been financed by CONACYT [grant number: 731862]

References

- [1] Wang, F., Lv, S., Fu, C., & Zhang, C. (2017). The first-principles calculations on trigonal and hexagonal structures of BiFeO₃. *Ferroelectrics*, 520(1), 177-18. <https://doi.org/10.1080/00150193.2017.1388763>
- [2] Chen, G., Chen, J., Pei, W., Lu, Y., Zhang, Q., Zhang, Q., & He, Y. (2019). Bismuth ferrite materials for solar cells: current status and prospects. *Materials Research Bulletin*, 110, 39-49. <https://doi.org/10.1016/j.materresbull.2018.10.011>
- [3] Heo, Y., & Alexe, M. (2022). Boosting Piezoelectricity under Illumination via the Bulk Photovoltaic Effect and the Schottky Barrier Effect in BiFeO₃. *Advanced Materials*, 34(5), 2105845. <https://doi.org/10.1002/adma.202105845>
- [4] Yang, T., Wei, J., Sun, Z., Li, Y., Liu, Z., Xu, Y., ... & Cheng, Z. (2022). Design of oxygen vacancy in BiFeO₃-based films for higher photovoltaic performance. *Applied Surface Science*, 575, 151713. <https://doi.org/10.1016/j.apsusc.2021.151713>
- [5] Wu, J., Fan, Z., Xiao, D., Zhu, J., & Wang, J. (2016). Multiferroic bismuth ferrite-based materials for multifunctional applications: ceramic bulks, thin films and nanostructures. *Progress in Materials Science*, 84, 335-402. <https://doi.org/10.1016/j.pmatsci.2016.09.001>
- [6] Razad, P. M., Saravanakumar, K., Ganesan, V., Choudhary, R. J., Moses Ezhil Raj, A., Devaraj, R., ... & Sanjeeviraja, C. (2017). Novel report on single phase BiFeO₃ nanorod layer synthesised rapidly by novel hot-wall spray pyrolysis system: evidence of high magnetization due to surface spins. *Journal of Materials Science: Materials in Electronics*, 28(4), 3217-3225. <https://doi.org/10.1007/s10854-016-5911-5>
- [7] Mori, T. J., Mouls, C. L., Morgado, F. F., Schio, P., & Cezar, J. C. (2017). Parasitic phases at the origin of magnetic moment in BiFeO₃ thin films grown by low deposition rate RF sputtering. *Journal of Applied Physics*, 122(12), 124102. <https://doi.org/10.1063/1.5003764>
- [8] Margha, F. H., Radwan, E. K., Badawy, M. I., & Gad-Allah, T. A. (2020). Bi₂O₃-BiFeO₃ glass-ceramic: controllable β-/γ-Bi₂O₃ transformation and application as magnetic solar-driven photocatalyst for water decontamination. *ACS omega*, 5(24), 14625-14634. <https://doi.org/10.1021/acsomega.0c01307>
- [9] Ryu, J., Baek, C. W., Park, D. S., & Jeong, D. Y. (2010). Multiferroic BiFeO₃ thick film fabrication by aerosol deposition. *Metals and Materials International*, 16(4), 639-642. <https://doi.org/10.1007/s12540-010-0818-9>

- [10] Afzal, A. M., Umair, M., Dastgeer, G., Rizwan, M., Yaqoob, M. Z., Rashid, R., & Munir, H. S. (2016). Effect of O-vacancies on magnetic properties of bismuth ferrite nanoparticles by solution evaporation method. *Journal of Magnetism and Magnetic Materials*, 399, 77-80. <https://doi.org/10.1016/j.jmmm.2015.09.062>
- [11] Jamil, H., Dildar, I. M., Ilyas, U., Hashmi, J. Z., Shaukat, S., Sarwar, M. N., & Khaleeq-ur-Rahman, M. (2021). Microstructural and Optical study of polycrystalline manganese oxide films using Kubelka-Munk function. *Thin Solid Films*, 732, 138796. <https://doi.org/10.1016/j.tsf.2021.138796>
- [12] Liang, K. Y., Wang, Y. F., Yang, Z., Zhang, S. P., Jia, S. Y., & Zeng, J. H. (2021). Above-Band-Gap Voltage from Oriented Bismuth Ferrite Ceramic Photovoltaic Cells. *ACS Applied Energy Materials*, 4(11), 12703-12708. <https://doi.org/10.1021/acsaem.1c02395>
- [13] Yan, X., Pu, R., Xie, R., Zhang, B., Shi, Y., Liu, W., ... & Yang, N. (2021). Design and fabrication of Bi₂O₃/BiFeO₃ heterojunction film with improved photoelectrochemical performance. *Applied Surface Science*, 552, 149442. <https://doi.org/10.1016/j.apsusc.2021.149442>
- [14] Duan, F., Ma, Y., Lv, P., Sheng, J., Lu, S., Zhu, H., ... & Chen, M. (2021). Oxygen vacancy-enriched Bi₂O₃/BiFeO₃ pn heterojunction nanofibers with highly efficient photocatalytic activity under visible light irradiation. *Applied Surface Science*, 562, 150171. <https://doi.org/10.1016/j.apsusc.2021.150171>
- [15] Nikumaa, M. (2011). Solid solution in the systems BiMO₃-ATiO₃ (M= Fe, Cr; A= Ba, Sr) synthesis, structure and magnetic properties (Master's thesis). <https://hdl.handle.net/20.500.12380/146774>
- [16] Ma, Y., Lv, P., Duan, F., Sheng, J., Lu, S., Zhu, H., ... & Chen, M. (2020). Direct Z-scheme Bi₂S₃/BiFeO₃ heterojunction nanofibers with enhanced photocatalytic activity. *Journal of Alloys and Compounds*, 834, 155158. <https://doi.org/10.1016/j.jallcom.2020.155158>
- [17] Yang, T., Wei, J., Guo, Y., Lv, Z., Xu, Z., & Cheng, Z. (2019). Manipulation of oxygen vacancy for high photovoltaic output in bismuth ferrite films. *ACS applied materials & interfaces*, 11(26), 23372-23381. <https://doi.org/10.1021/acsami.9b06704>